frontiers | Frontiers in Earth Science

ORIGINAL RESEARCH
published: 27 April 2022
doi: 10.3389/feart.2022.857260

Sedimentary $CaCO_3$ Accumulation in the Deep West Pacific Ocean

Handan Zhang[1,2,3†], *Hong Che*[4†], *Jinqi Xia*[1], *Qi Cheng*[1], *Di Qi*[5], *Junqian Cao*[1] *and Yiming Luo*[1,2,3*]

[1]School of Marine Sciences, Sun Yat-Sen University, Zhuhai, China, [2]Southern Marine Science and Engineering Guangdong Laboratory (Zhuhai), Guangdong, China, [3]Guangdong Provincial Key Laboratory of Marine Resources and Coastal Engineering, Guangzhou, China, [4]Pilot National Laboratory for Marine Science and Technology, Qingdao, China, [5]Polar and Marine Research Institute, College of Harbor and Coastal Engineering, Jimei University, Xiamen, China

Distribution of calcium carbonate ($CaCO_3$) in marine sediment has been studied over the last century, and influence by multiple factors with regard to dissolution and dilution of sedimentary $CaCO_3$ has long been established. There is still lack of quantification on the influence of those factors, so it remains elusive to determine which specific process is driving the down-core variation of $CaCO_3$ content ($_{wt}CaCO_3$%) records. Here, based on a newly compiled $CaCO_3$ data set and a carbonate model, depth-profiles of sedimentary $_{wt}CaCO_3$% from the West Pacific Ocean can be well illustrated, and influence from different factors on their distribution features can be quantified. The deep ocean circulation is found to largely shape the inter-basin disparity in sedimentary $_{wt}CaCO_3$% distribution between the equatorial regions (e.g., the Western Equatorial Pacific Ocean and the Central Pacific Ocean) and the north–west regions (the Philippine Sea and the Northwest Pacific Ocean) in our study region. Moreover, the slow carbonate dissolution rate in the deep Central Pacific Ocean guarantees better accumulation of $CaCO_3$ at depth compared to that in other regions. However, enhanced dilution by non-carbonate materials of sedimentary $CaCO_3$ on a topographic complex can potentially obstruct the dissolution profiles constituted by sedimentary $_{wt}CaCO_3$% in the pelagic ocean. The aforementioned assertion suggests that changes of $_{wt}CaCO_3$% accumulation in marine sediment in the West Pacific Ocean can be used to dictate past changes of the deep ocean circulation (2,500 to 3,000 m) in this area but constraint on the non-carbonate flux, especially on the topographic complex, should be necessary.

Keywords: surface sediment, overturning circulation, non-carbonate dilution, $CaCO_3$, Western Pacific

OPEN ACCESS

Edited by:
Xiting Liu,
Ocean University of China, China

Reviewed by:
Jun Tian,
Tongji University, China
Zhaojie Yu,
Institute of Oceanology (CAS), China

***Correspondence:**
Yiming Luo
luoyiming@mail.sysu.edu.cn

†These authors have contributed equally to this work

Specialty section:
This article was submitted to Marine Geoscience, a section of the journal Frontiers in Earth Science

Received: *18 January 2022*
Accepted: *28 March 2022*
Published: *27 April 2022*

Citation:
Zhang H, Che H, Xia J, Cheng Q, Qi D, Cao J and Luo Y (2022) Sedimentary $CaCO_3$ Accumulation in the Deep West Pacific Ocean. Front. Earth Sci. 10:857260. doi: 10.3389/feart.2022.857260

INTRODUCTION

The global ocean is actively involved in the climate regulation by influencing the carbon cycling on the Earth's surface on different time scales (Regnier et al., 2013). Processes governing the carbon sequestration from the lower atmosphere to the ocean and cycles of carbon in the ocean interior are mainly known as the biological pump and the solubility/physical pump, respectively. In particular, the biological pump transforms dissolved inorganic carbon into particulate organic carbon in the surface ocean, transfers the particulate organic carbon (POC) to depth via settling particles, and releases the sequestrated carbon back into the sea water as CO_2 by microbial metabolism/respiration (POC remineralization) (Volk and Hoffert, 1985). In contrast, the solubility/physical pump regulates carbon partition between the lower atmosphere and the surface ocean by CO_2 exchange (Ito and

Follows, 2003), transports carbon from the surface ocean to the deep ocean by deep convection (deep water formation), and circulates carbon in deep ocean basins by the global ocean conveyor belt (thermohaline circulation).

The Pacific Ocean, which is the biggest marine carbon reservoir at the end of the global ocean conveyor belt, hosts the oldest and carbon-rich deep water in the global ocean owing to accumulated organic matter remineralization (Yu et al., 2020). The corrosive Pacific deep water (Sexton and Barker, 2012) results in shallower preservation depth of calcite (rarer and more soluble aragonite is excluded in our analysis), which hereafter is the only carbonate mineral considered in this article, in the Pacific sediments than that in the Atlantic and Indian ocean sediments (Berger et al., 1976; Biscaye et al., 1976; Kolla et al., 1976). Features regarding the spatial distribution of Pacific sedimentary $CaCO_3$ content ($_{wt}CaCO_3$%) have long been discovered to be related to multiple factors (e.g., ocean productivity, ocean circulation, and lithogenic dilution), while their impacts have not been quantified (Broecker, 2008). Given the importance of the Pacific Ocean in the global carbon cycle, especially during the climate transition periods (e.g., the suggested CO_2 outgassing way to the atmosphere from the abyss during the last deglaciation; Gray et al., 2018), it is necessary to conduct a quantitative assessment on the carbonate distribution in the deep Pacific Ocean, in order to establish the basis to examine past changes of the Pacific carbonate system.

Sedimentary $CaCO_3$ in the deep sea mainly consists of calcite or aragonite sourced from calcifying plankton. Theoretically, the upper water column of the ocean is saturated with regard to $CaCO_3$, and critical dissolution of calcite takes place below a horizon where the sea water becomes calcite-under-saturated as a result of increased solubility of calcite with water depth (pressure). Under-saturation of $CaCO_3$ could be generated in the micro-environment above the general carbonate saturation horizon as a result of intense POC respiration. Therefore, dissolution of the more soluble aragonite could happen in the upper water column, which is not considered in this current study. Generally, profiles of sedimentary calcite content versus water depth exhibit classic $CaCO_3$-depth features (Chung et al., 2003) with high constant values of $_{wt}CaCO_3$% at shallower depths and a systematic decrease below the calcite saturation horizon to reach essentially zero content at deeper depths (Broecker and Peng, 1982).

However, plotting the surficial sedimentary $_{wt}CaCO_3$% versus water depth in the Pacific Ocean gives a data cloud (**Supplementary Figure S1**). Although the decrease of $_{wt}CaCO_3$% with water depth below ~3,000 m can be illustrated, the trend is rather unrefined to provide any informative message. The reason is that the dynamic ecology (i.e., $CaCO_3$ export productivity) in the surface of the Pacific Ocean and complexity in the deep ocean (i.e., topography, submarine volcano, and circulation, etc.) bring uncertainties to the sedimentary $CaCO_3$ distribution, which demands sub-grouping of the data to distinguish the influence of such processes.

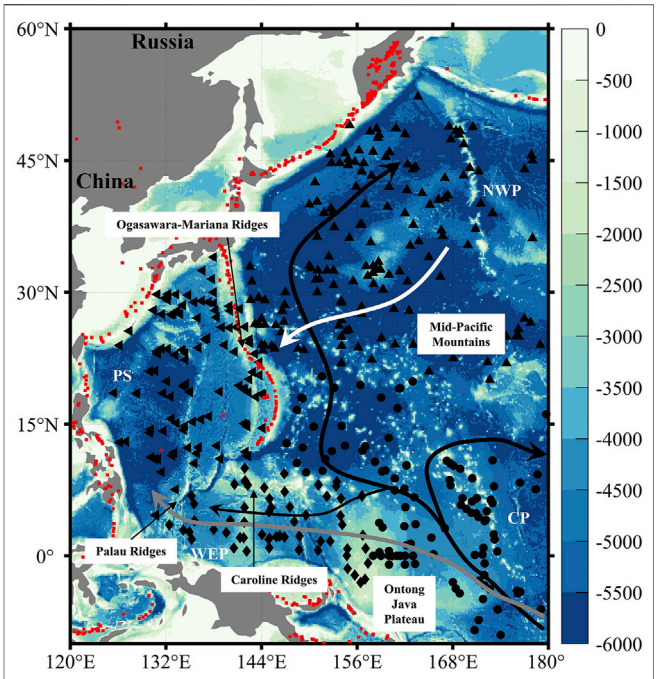

FIGURE 1 | Map of the study region with black markers representing the locations of sediment cores (triangle—the Northwest Pacific; left triangle—the Philippine Sea; diamond—the Western Equatorial Pacific; circle—the Central Pacific) (see **Supplementary Table S1**). White, gray, and black arrows show the pathway of the major deep thermohaline currents (e.g., the North Pacific Deep Water (NPDW), the Upper Circumpolar Deep Water (UCDW), and the Lower Circumpolar Deep Water (LCDW)) in the Pacific Ocean (Johnson and Toole, 1993; Kawabe et al., 2003; Fiedler and Talley, 2006; Kawabe and Fujio, 2010). Red rhombus represents major volcanoes and hydrothermal vents in the Pacific Ocean (Beaulieu, 2010; Venzke, 2013).

This current study is therefore carried out in order to understand the underlying mechanism of $CaCO_3$ accumulation in the West Pacific Ocean by re-analyzing compiled surficial sedimentary $CaCO_3$ distribution patterns. Our work provides a quantitative constraint of the geographical variations in sedimentary $_{wt}CaCO_3$% distribution in the West Pacific Ocean, which will help to establish a way to constrain the deep ocean circulation and uncover the role of the West Pacific Ocean in global carbon cycles in the geological past.

METHODS AND THEORETICAL MODEL

The Study Area

The intricate bottom topography (i.e., widely distributed seamounts and guyots) of the West Pacific Ocean results in complicated distributions of different thermohaline currents. The deep water below about 3,500 m in the West Pacific Ocean is dominated by the Lower Circumpolar Deep Water (LCDW), which flows northward along the Chatham Rise in the western South Pacific Ocean (Chiswell et al., 2015) and enters the Central Pacific Ocean through the Samoan Passage, where it bifurcates into western, northern, and eastern branches (**Figure 1**) (Johnson and Toole, 1993; Kawabe et al., 2003;

TABLE 1 | Predicted values of the carbonate saturation depth (CSD), carbonate dissolution rate (k*), and non-carbonate flux (F_M) obtained from parameters of PIC flux (F_B), [CO_3^{2-}] (spatial mean value ± standard deviation), and observed carbonate compensation depth (CCD) used in the control run.

Region	Northwest Pacific Ocean	Philippine Sea	Western Equatorial Pacific Ocean	Central Pacific Ocean
[CO_3^{2-}] (μmol kg^{-1})	68.2 ± 5.5	71.1 ± 3.8	73.7 ± 3.4	74.9 ± 3.7
F_B (g m^{-2} yr^{-1})	7.0 ± 1.4	6.5 ± 0.2	13.0 ± 0.2	8.0 ± 0.5
Observed CCD (m)	4,000 ± 300	4,100 ± 300	4,500 ± 400	5,100 ± 400
CSD (m)	2,420	2,650	2,820	2,910
F_M (g m^{-2} yr^{-1})	0.97	0.84	2.4	1.2
k* (m yr^{-1})	2.95 (2.35–3.74)	2.89 (2.31–3.72)	4.79 (3.68–6.54)	2.09 (1.69–2.65)

Kawabe and Fujio, 2010). The Upper Circumpolar Deep Water (UCDW), originated from the Antarctic Circumpolar Current (ACC), is transported by the anticyclonic flow at shallower depths through the South Pacific and ultimately enters the Philippine Sea via the Caroline Basin (**Figure 1**) (Kawabe et al., 2003). Upwelled LCDW in the Northeast Pacific Ocean is transformed into another upper deep water, the North Pacific Deep Water (NPDW), between 2,000 and 3,500 m, which is modified on its southward route by mixing with UCDW.

The LCDW fills the deep ocean below about 3,500 m mainly in the West Pacific Ocean (**Supplementary Figure S1**), producing a relatively young water mass age (500–700 years) in the Central Pacific Basin and older water mass age in the Caroline, Philippine, and North Pacific basins (700–1,000 years) between 3,500 m and 4,000 m, coinciding with the decreasing carbonate ion ([CO_3^{2-}]) from the Central Pacific Ocean to the Northwest Pacific Ocean as a result of accumulated respiration of organic matter (**Supplementary Figures S2, S4**). Ages of the water mass and [CO_3^{2-}] at a depth between 2,500 m and 3,000 m, where UCDW dominates, show weaker inter-basin contrast, but aging of the water mass (decreasing [CO_3^{2-}]) from the South to the North can still be found in our study region (**Supplementary Figures S3, S4**).

Data Preparation

Data used in this study include surficial $CaCO_3$ content in sediments ($_{wt}CaCO_3$%), carbonate ion concentration in the deep ocean ([CO_3^{2-}]), PIC rain (F_B), and non-carbonate flux (F_M).

Surficial sedimentary $_{wt}CaCO_3$% data used in this article are compiled from previously published references, with details appended in **Supplementary Table S1**. Sediment cores from the West Pacific Ocean are separated into four geographic groups (e.g., the Northwest Pacific Ocean, the Philippine Sea, the Western Equatorial Pacific Ocean (including mostly the Caroline Basin), and the Central Pacific Ocean). The topographic complex in the deep ocean (e.g., the Ogasawara–Mariana–Palau Ridges, the Caroline Ridges, the Ontong Java Plateau, and the Mid-Pacific Mountains) sets the boundary between different regions (**Figure 1**), and measured carbonate chemistry (GLODAPv2.2020; Olsen et al., 2020) and simulated deep water-mass ages by the Norwegian Earth System Model (NorESM; Tjiputra et al., 2013) differ among the four regions (**Supplementary Figures S2, S3**). Carbonate ion concentration ([CO_3^{2-}]) data used in this study were calculated from titration alkalinity, total dissolved inorganic carbon, salinity, temperature, and pressure (water depth) data obtained from the Global Ocean Data Analysis Project version 2.2020 database (GLODAPv2.2020; Millero, 1995; Olsen et al., 2020). A basin-wide distribution of the deep sea [CO_3^{2-}] below 1,000 m is illustrated in **Supplementary Figure S4**, with average values between 2,000 and 3,000 m for different ocean regions and the *in situ* variance summarized in **Table 1**.

Rain (flux) of particulate inorganic carbon (PIC; F_B) to the surficial sediment consists mostly settling $CaCO_3$ produced in the surface ocean by marine calcifiers. To calculate the PIC rain, the net primary production was first estimated (**Supplementary Figure S5A**) using the monthly Moderate Resolution Imaging Spectroradiometer (MODIS) datasets based on a carbon-based production model (CBPM; Behrenfeld et al., 2005), which is then translated into the export flux of particulate organic carbon (POC; **Supplementary Figure S5B**) using algorithms developed by Laws et al. (2000).The export flux of PIC is then derived based on the PIC:POC export ratio (Sarmiento et al., 2002), and the PIC rain (**Table 1**) is assigned to be half of the export flux of PIC due to carbonate dissolution in the water column as a result of POC remineralization (Feely et al., 2004). Dilution of marine $CaCO_3$ in the pelagic ocean is largely determined by non-carbonate components, such as lithogenic materials and biogenic opal, despite dominant fluvial input to ocean margins. As the major source for lithogenic input (F_M), eolian dust is estimated by various means (Kienast et al., 2016), and the results are shown in **Supplementary Table S2**. In particular, model simulated dust deposition (**Supplementary Figure S6**; Jickells et al., 2005) suggests that the Northwest Pacific Ocean has the highest mean dust deposition at about 0.97 g m^{-2} yr^{-1}, and dust deposition in other areas ranges from ~0.2 g m^{-2} yr^{-1} (the Central Pacific Ocean and the Western Equatorial Pacific Ocean) to ~0.84 g m^{-2} yr^{-1} (the Philippine Sea).

Carbonate Accumulation Model

To better constrain the observed sedimentary $_{wt}CaCO_3$% distribution, a critical depth where $CaCO_3$ turns under-saturated beneath (the carbonate saturation depth; CSD) is first calculated from [CO_3^{2-}] in the deep ocean between 2,500 m and 3,000 m in different basins, where the sea water turns under-saturated (**Supplementary Figure S4**), based on empirical relationships established by Boudreau et al. (2010). Another critical depth where the carbonate sedimentation rate

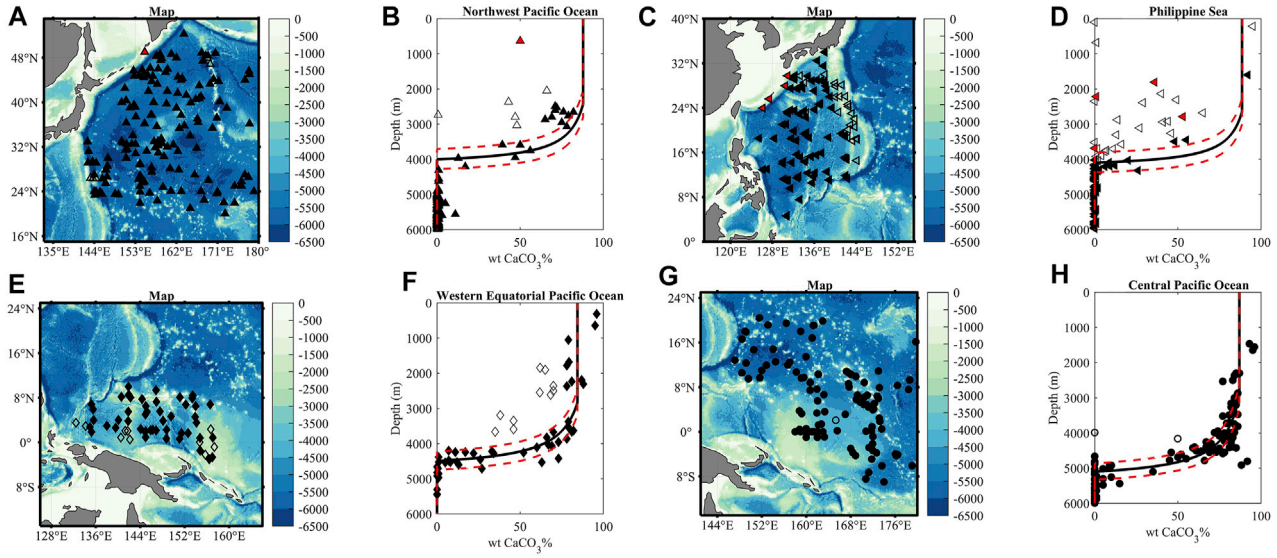

FIGURE 2 | Location of the sampling sites and distributions of sedimentary $CaCO_3$ in the Northwest Pacific Ocean [triangles; **(A,B)**], Philippine Sea [left triangles; **(C,D)**], Western Equatorial Pacific Ocean [diamonds; **(E,F)**], and Central Pacific Ocean [circles; **(G,H)**]. Pelagic sediments with high $CaCO_3$ content presumably not strongly affected by non-carbonate dilution are marked by filled black symbols, while those with low $CaCO_3$ content are marked by unfilled black symbols. Samples from ocean margins with low $CaCO_3$ content are labeled in red [panels **(A–D)**]. The solid black lines are model outputs (control runs) for the pelagic Northwest Pacific Ocean **(A)**, Philippine Sea **(B)**, Western Equatorial Pacific Ocean **(C)**, and Central Pacific Ocean. The sensitivity tests with $[CO_3^{2-}]$ (±~5 μmol kg^{-1}) are presented by the red dashed line.

balances its dissolution rate (the carbonate compensation depth; CCD) can be determined by finding the depth, below which no accumulation of $CaCO_3$ could be found. Observed locations of CCD can be used to derive values of the dissolution rate of $CaCO_3$ (k*; **Table 1**) with the PIC rain (F_B), deep sea $[CO_3^{2-}]$, and non-carbonate flux (F_M) (Li et al., 2021; Liu et al., 2022).

Ultimately, the sedimentary $_{wt}CaCO_3$% (B) at a given water depth between CSD and CCD can be calculated by:

$$B = \frac{F_B - k^*\left([CO_3^{2-}]_{sat} - [CO_3^{2-}]\right)}{\left(F_B - k^*\left([CO_3^{2-}]_{sat} - [CO_3^{2-}]\right)\right) + \left(\rho_{CaCO_3} F_M / \rho_M\right)}, \quad (1)$$

where ρ_{CaCO3} is the mass density of $CaCO_3$ (2.5×10^4 mol m^{-3}; Boudreau, 2013), ρ_M is the density of non-carbonate sediment (2.5×10^6 g m^3; Archer, 1996), F_B is the PIC rain (mol m^{-2} yr^{-1}), $[CO_3^{2-}]$ and $[CO_3^{2-}]_{sat}$ are deep-sea carbonate ion and deep-sea carbonate ion at saturation, respectively, and F_M is the non-carbonate flux (g m^{-2} yr^{-1}), which can be calculated from observed constant sedimentary $_{wt}CaCO_3$% (B) above the CSD (Liu et al., 2022; **Supplementary Table S2**).

RESULTS

Sedimentary $CaCO_3$ Distributions

Locations of the samples and distributions of sedimentary $CaCO_3$ in different ocean regions are shown in **Figure 2**. The deposition depth of marine $CaCO_3$ is relatively shallow in the Northwest Pacific Ocean and the Philippine Sea. Pelagic sediments in the Northwest Pacific have 70%–80% $_{wt}CaCO_3$ at ~2,500 m, below which $_{wt}CaCO_3$% decreases to zero at ~4,000 m (black triangles in **Figures 2A,B**). In the pelagic Philippine Sea, sedimentary $_{wt}CaCO_3$% decreases with a water depth from ~92% at ~1,600 m, and almost no $CaCO_3$ can be found in sediments at depths below ~4,100 m (filled black left triangles in **Figures 2C,D**), with most of sedimentary $_{wt}CaCO_3$% data between 2,000 m and 4,000 m from core-tops retrieved on the Ogasawara–Mariana and Kyushu–Palau ridges (unfilled left triangles in **Figures 2C,D**). The sedimentary $CaCO_3$ distribution in the Western Equatorial Pacific Ocean (diamonds) and the Central Pacific Ocean (circles) is presented in **Figures 2E–H**, with sedimentary $_{wt}CaCO_3$% decreasing below ~3,000 m with depths to reach zero at ~4,500 m and ~5,200 m, respectively.

Model Outputs

Features in observed $CaCO_3$-depth profiles can be largely reproduced by our model using parameters listed in **Table 1**. The predicted positions of CSD for different regions generally correspond to where the first systematic decrease of sedimentary $_{wt}CaCO_3$% can be observed (**Figure 2**). The CSD is the deepest in the Central Pacific Ocean (~2,900 m) with a slight shoaling to ~2,800 m in the Western Equatorial Pacific Ocean and ~2,700 m in the Philippine Sea. The CSD is the shallowest (~2,300 m) in the Northwest Pacific Ocean. Such results are based on measured deep-sea $[CO_3^{2-}]$ averaged over 300 m above the sea floor for depths between 2,500 m and 3,000 m, obtained from GLODAPv2-2020 data (**Supplementary Figure S4**; Olsen et al., 2020). The dissolution rate of $CaCO_3$ (k*) calculated based on observed values of CCD is on the same order of magnitude among

sediments from different regions of the West Pacific Ocean (**Table 1**), with a relatively low k* (~2 m yr^{-1}) for the Central Pacific Ocean, a high k* (~5 m yr^{-1}) for the Western Equatorial Pacific Ocean, and medium k* (~3 m yr^{-1}) for other regions.

The predicted $CaCO_3$-depth profiles (solid lines in **Figure 2**) from our model can reproduce the general patterns of observed sedimentary $CaCO_3$ distribution across different domains, despite some data points deviated from the depth-$CaCO_3$ profiles and uncertainties associated with the sedimentary $_{wt}CaCO_3$% data that will be addressed later. A comparison between the measured $_{wt}CaCO_3$% data and model outputs (control runs) suggests that model simulations are statistically consistent with the actual data (**Supplementary Figure S7**).

DISCUSSION

Influence of Deep Ventilation on the Sedimentary $CaCO_3$ Distribution

Intrusion of the LCDW and UCDW originated from the Southern Ocean into the Central Pacific Basin results in relatively higher dissolved [CO_3^{2-}] (~75 μmol kg^{-1}) below 2,000 m than other regions in the West Pacific Ocean (**Supplementary Figures S3, S4**). Therefore, the deep water in the Central Pacific Basin is relatively carbonate saturated so that $CaCO_3$ can be better preserved at depths. Aging of the UCDW and a branch of the LCDW that enters the Western Equatorial Pacific Ocean do not integrate enough with effect of POC remineralization with time in the Western Equatorial Pacific Ocean so that the regional deep-sea [CO_3^{2-}] in the deep Western Equatorial Pacific Ocean (~74 μmol kg^{-1}) remains close to that in the Central Pacific Ocean. The deep water in the Philippine Sea is largely controlled by the UCDW since direct intrusion of the younger and deeper LCDW is restricted by the island chains, which leads to lower deep-sea [CO_3^{2-}] (~71 μmol kg^{-1}) than that in the deep Western Equatorial Pacific Ocean. Further north, weakening of LCDW with a volume transport of 12–14 Sv (10^6 m^3 s^{-1}) in the Central Pacific Ocean to 6 Sv in the Northwest Pacific Ocean (Kawabe and Fujio, 2010), as well as enhanced control of the North Pacific Deep Water (NPDW) in the Northwest Pacific Ocean, is in coincidence with a distinct decline of [CO_3^{2-}] (~68 μmol kg^{-1}) compared to other regions and shallow saturation depth of sedimentary $CaCO_3$ (2,420 m; **Figure 2**; **Table 1**).

To counteract the increasing T_{CO2} resulted from accumulated organic matter respiration with time and compensate for the loss of [CO_3^{2-}], carbonate dissolution takes place at shallower ocean depths as the deep water ages (**Figures 2**; **Supplementary Figure S4**). Therefore, the contrasting features of sedimentary $CaCO_3$ between the equatorial regions (e.g., the Western Equatorial Pacific Ocean and the Central Pacific Ocean) and the northwest regions (the Philippine Sea and the Northwest Pacific Ocean) in our study region can be attributed to patterns of the abyssal circulation. Below the carbonate saturation depth, accumulation of $CaCO_3$ in marine sediments is determined by the rate of carbonate dissolution (k*) (Boudreau et al., 2020). The approach we take can help to estimate the basin-scale-averaged carbonate dissolution rate (k*) in the West Pacific Ocean, which seems to be in concert with k* based on water-side control

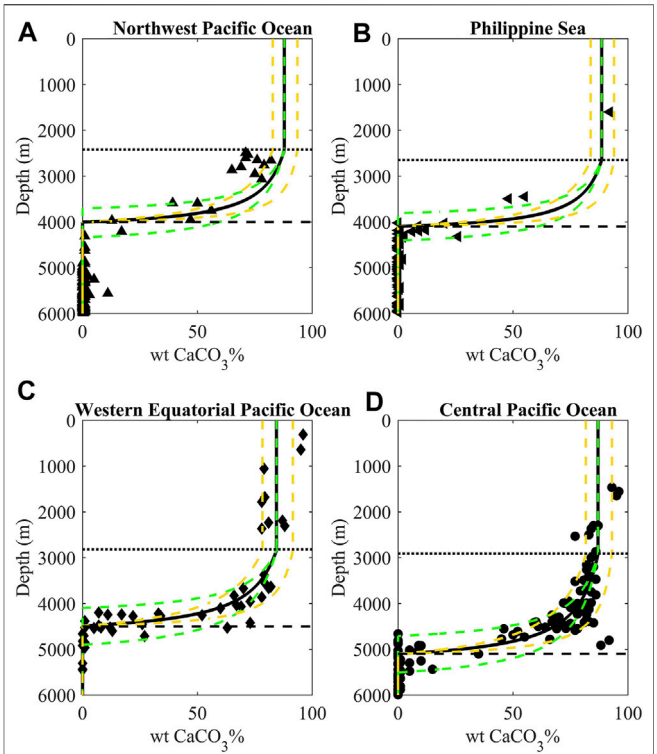

FIGURE 3 | Pelagic sedimentary $_{wt}CaCO_3$%-depth profiles and model outputs for the Northwest Pacific Ocean **(A)**, Philippine Sea **(B)**, Western Equatorial Pacific Ocean **(C)**, and Central Pacific Ocean **(D)**. Predictions by the model's control run (**Table 1**) are shown by bold black lines. The sensitivity tests with observed position of carbonate compensation depth (±400 m, with corresponding uncertainty of the carbonate dissolution rate k*) and non-carbonate fluxes F_M (±50%) are presented by green and golden dashed lines, respectively. The carbonate saturation depth (CSD) and carbonate compensation depth (CCD) are indicated by the black dotted and dashed lines, respectively.

(**Table 1**; Sulpis et al., 2018), consistent with our previous estimation of k* in the Southwestern Atlantic Ocean and marginal seas in the western Pacific Ocean (Li et al., 2021; Liu et al., 2022). Therefore, our calculation is in support of the assertion that carbonate dissolution is mainly controlled by diffusion through the diffusion boundary layer (Boudreau et al., 2020).

With the lowest k* (~2 m yr^{-1}) among different regions in the West Pacific Ocean, $CaCO_3$ dissolves slow in under-saturated deep waters in the Central Pacific Ocean so that more $CaCO_3$ can get accumulated in sediment at a deeper depth. In contrast, the high k* (~5 m yr^{-1}) in the Western Equatorial Pacific Ocean infers fast $CaCO_3$ dissolution, and $CaCO_3$ can get accumulated in sediment at a much shallower depth compared to that in the Central Pacific Ocean, though the PIC rain in the Western Equatorial Pacific Ocean is doubling that in the Central Pacific Ocean. The rate of carbonate dissolution (k*) due to water-side control is determined by the rate of deep current, and our derived high k* in the Western Equatorial Pacific Ocean and low k* in the Central Pacific Ocean are in line with high bottom current speed in the Western Equatorial Pacific Ocean and low bottom current speed in the Central Pacific Ocean (Sulpis et al., 2018).

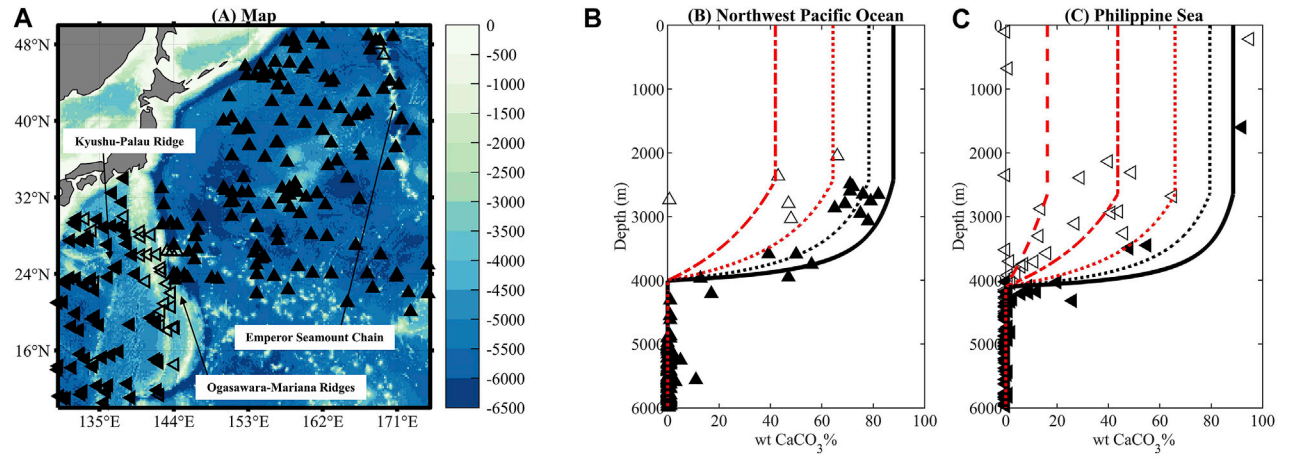

FIGURE 4 | Map **(A)** detailing ridges in the West Pacific Ocean and **(B)** plots of sedimentary $_{wt}CaCO_3$% versus depth in the Philippine Sea and the Northwest Pacific Ocean. Pelagic sediments with high $CaCO_3$ content presumably not strongly affected by non-carbonate dilution are marked by filled black symbols, while those with low $CaCO_3$ content from the Emperor Seamount Chain, the Ogasawara–Mariana Ridge, and Kyushu–Palau Ridge are marked by unfilled black symbols. The solid black lines are model outputs (control runs) for the pelagic Northwest Pacific Ocean **(B)** and Philippine Sea **(C)**. The black dotted, red dotted, dot and dash, and dashed lines show sensitivity tests with 2, 4, 10, and 40 times of F_M, respectively.

Influence of Non-Carbonate Dilution

It is worth mentioning that the uncertainty in regional [CO_3^{2-}] or observed location of CCD cannot fully account for the variability of basinal sedimentary $_{wt}CaCO_3$% distribution (**Figures 2**, **3**). The sedimentary $_{wt}CaCO_3$% above the carbonate saturation depth in both the Western Equatorial Pacific Ocean and the Central Pacific Ocean shows strong regional variability (**Figure 3**), which could either be caused by different *in situ* PIC rain (F_B) or varied dilution intensity of the non-carbonate flux (F_M). The estimated PIC rain (F_B; **Table 1**) in the Western Equatorial Pacific Ocean is more than doubling that in the Central Pacific Ocean. However, the sedimentary $_{wt}CaCO_3$% above the CSD in the Western Equatorial Pacific Ocean is not higher than that in the Central Pacific Ocean, suggesting non-carbonate materials in sediments is playing an important role in determining $_{wt}CaCO_3$%.

Calculated fluxes of non-carbonate materials (F_M) are high in the Western Equatorial Pacific Ocean (~2.4 g m^{-2} yr^{-1}), which is generally in agreement with the high flux of non-carbonate materials recorded by sediment traps but remarkably higher than simulated dust deposition rates and Th-derived lithogenic flux (**Supplementary Figure S6**; **Supplementary Table S2**). Such a comparison indicates that lithogenic input alone is not sufficient to account for the carbonate dilution in the Western Equatorial Pacific Ocean. Alternatively, high fluxes of biogenic opal with spatial disparity in the Western Equatorial Pacific Ocean, and perhaps in the equatorial upwelling region in the Central Pacific Ocean as well, could have contributed to the dilution of $CaCO_3$ in sediment.

Lack of sedimentary $_{wt}CaCO_3$% data above CSD in both the Northwest Pacific Ocean and the Philippine Sea hinders our constraint on the flux of non-carbonate materials in both basins. We thus take the dust deposition rates directly as lithogenic flux (F_M) in the model, and our model predictions of depth-profiles of sedimentary $_{wt}CaCO_3$% can reasonably reproduce the scarce sedimentary $_{wt}CaCO_3$% data from the two regions, despite lower sedimentary $_{wt}CaCO_3$% data between 2,000 m and 4,000 m from core-tops retrieved mostly on the Ogasawara–Mariana and Kyushu–Palau ridges (unfilled symbols in **Figure 2**). It is worth mentioning that Th-derived lithogenic flux in the Northwest Pacific Ocean is 1–4 times higher than the rate of dust deposition (**Supplementary Table S2**), and such a magnitude of increase of F_M suffices to reproduce the low sedimentary $_{wt}CaCO_3$% in the pelagic Northwest Pacific Ocean between 2,500 m and 3,600 m (**Figure 4**).

Sediment-trap-recorded flux of non-carbonate materials in the Northwest Pacific Ocean is 6–20 times higher than the rate of dust deposition (**Supplementary Table S2**) due to contribution of biogenic opal (Kawahata et al., 1998). Therefore, the spatial variance in the flux of biogenic opal in the Northwest Pacific Ocean could potentially explain some of the low $_{wt}CaCO_3$% found in sediment on the Emperor Seamount Chain. However, trap-recorded flux in the oligotrophic Philippine Sea is only 1–2 times higher than the dust deposition rate (**Supplementary Table S2**; Kawahata et al., 1998), and such uncertainty could not explain the diluted sedimentary $_{wt}CaCO_3$% in that region (**Figure 4C**). To reproduce the low sedimentary $_{wt}CaCO_3$% from the Ogasawara–Mariana and Kyushu–Palau ridges, one needs 2–40 times higher flux of non-carbonate materials than the dust deposition rate, which could only be attributed to detritus derived from volcanic activities in this area.

CONCLUSION

Patterns of accumulated $CaCO_3$ in sediment in the West Pacific Ocean have been revisited. With a simple carbonate accumulation model applied, factors that could exert influence on the sedimentary $CaCO_3$ distribution have been examined. Notwithstanding uncertainties associated with the factors that must account for variability in sedimentary

$_{wt}CaCO_3$%, the deep ventilation (a.k.a. thermohaline currents) substantially shapes the depth-profiles of sedimentary $CaCO_3$ in different regions in the West Pacific domain. Furthermore, the dominant control of carbonate dissolution by diffusion through the diffusion boundary layer is verified using our approach, which is in line with the control of deep ocean ventilation on sedimentary $CaCO_3$ distribution. Enhanced dilution by non-carbonate materials of sedimentary $CaCO_3$ on the topographic complex is uncovered, which can potentially obstruct the dissolution profiles constituted by sedimentary $_{wt}CaCO_3$% in the pelagic ocean. Given that the variation of the non-carbonate flux on the topographic complex can be properly constrained, our results imply that the basinal sedimentary $_{wt}CaCO_3$% distribution has the potential to reflect changes of the carbonate chemistry in the deep ocean (2,500 to 3,000 m) in the past, which could be associated with either changes of the property of UCDW or a mass replacement in the West Pacific Ocean. This information would then help us to dictate possible reorganization of the thermohaline circulation and understand the role the West Pacific Ocean played in global carbon cycles in the geological past.

DATA AVAILABILITY STATEMENT

The original contributions presented in the study are included in the article/**Supplementary Material**, further inquiries can be directed to the corresponding author.

AUTHOR CONTRIBUTIONS

YL conceived the study. YL, HC, HZ, and JX carried out data analysis. HZ and JX performed model simulations. YL and HC wrote the original draft. HZ, JX, DQ, QC, and JC participated in reviewing and editing the manuscript. All authors contributed to the final version of the manuscript.

FUNDING

This research was supported by the National Key Research and Development Program of China (2019YFE0114800), the National Natural Science Foundation of China (41976031 and 41976192), and Innovation Group Project of Southern Marine Science and Engineering Guangdong Laboratory (Zhuhai) (No. 311020005). YL acknowledges the support from the State Key Laboratory of Marine Geology, Tongji University (VF201810, MGK1908), the Key Laboratory of Global Change and Marine-Atmospheric Chemistry, MNR (GCMAC1803), and grant from the Open Foundation of Key Laboratory of Submarine Geosciences, MNR (KLSG1904).

SUPPLEMENTARY MATERIAL

The Supplementary Material for this article can be found online at: https://www.frontiersin.org/articles/10.3389/feart.2022.857260/full#supplementary-material

REFERENCES

Archer, D. E. (1996). An Atlas of the Distribution of Calcium Carbonate in Sediments of the Deep Sea. *Glob. Biogeochem. Cycles* 10 (1), 159–174. doi:10.1029/95gb03016

Beaulieu, S. (2010). InterRidge Global Database of Active Submarine Hydrothermal Vent fields: Prepared for InterRidge. Version 2.0. Available at: http://www.Interridge.Org/irvents.

Behrenfeld, M. J., Boss, E., Siegel, D. A., and Shea, D. M. (2005). Carbon-Based Ocean Productivity and Phytoplankton Physiology from Space. *Glob. Biogeochem. Cycles* 19 (1), GB1006. doi:10.1029/2004GB002299

Berger, W. H., Adelseck, C. G., Jr, and Mayer, L. A. (1976). Distribution of Carbonate in Surface Sediments of the Pacific Ocean. *J. Geophys. Res.* 81 (15), 2617–2627. doi:10.1029/JC081i015p02617

Biscaye, P. E., Kolla, V., and Turekian, K. K. (1976). Distribution of Calcium Carbonate in Surface Sediments of the Atlantic Ocean. *J. Geophys. Res.* 81 (15), 2595–2603. doi:10.1029/JC081i015p02595

Boudreau, B. P. (2013). Carbonate Dissolution Rates at the Deep Ocean Floor. *Geophys. Res. Lett.* 40 (4), 744–748. doi:10.1029/2012GL054231

Boudreau, B. P., Middelburg, J. J., and Meysman, F. J. R. (2010). Carbonate Compensation Dynamics. *Geophys. Res. Lett.* 37 (3), L03603. doi:10.1029/2009GL041847

Boudreau, B. P., Sulpis, O., and Mucci, A. (2020). Control of CaCO3 Dissolution at the Deep Seafloor and its Consequences. *Geochimica et Cosmochimica Acta* 268, 90–106. doi:10.1016/j.gca.2019.09.037

Broecker, W. S. (2008). A Need to Improve Reconstructions of the Fluctuations in the Calcite Compensation Depth over the Course of the Cenozoic. *Paleoceanography* 23 (1), PA1204. doi:10.1029/2007pa001456

Broecker, W. S., and Peng, T. H. (1982). "Tracers in the Sea," in *Lamon-Doherty Geological Observatory* (Palisades, NY: Coumbio University), 687.

Chiswell, S. M., Bostock, H. C., Sutton, P. J., and Williams, M. J. (2015). Physical Oceanography of the Deep Seas Around New Zealand: A Review. *New Zealand J. Mar. Freshw. Res.* 49 (2), 286–317. doi:10.1080/00288330.2014.992918

Chung, S.-N., Lee, K., Feely, R. A., Sabine, C. L., Millero, F. J., Wanninkhof, R., et al. (2003). Calcium Carbonate Budget in the Atlantic Ocean Based on Water Column Inorganic Carbon Chemistry. *Glob. Biogeochem. Cycles* 17 (4), 1093. doi:10.1029/2002GB002001

Feely, R. A., Sabine, C. L., Lee, K., Berelson, W., Kleypas, J., Fabry, V. J., et al. (2004). Impact of Anthropogenic CO2 on the CaCO3 System in the Oceans. *Science* 305 (5682), 362–366. doi:10.1126/science.1097329

Fiedler, P. C., and Talley, L. D. (2006). Hydrography of the Eastern Tropical Pacific: A Review. *Prog. Oceanography* 69 (2), 143–180. doi:10.1016/j.pocean.2006.03.008

Gray, W. R., Rae, J. W. B., Wills, R. C. J., Shevenell, A. E., Taylor, B., Burke, A., et al. (2018). Deglacial Upwelling, Productivity and CO2 Outgassing in the North Pacific Ocean. *Nat. Geosci* 11 (5), 340–344. doi:10.1038/s41561-018-0108-6

Ito, T., and Follows, M. J. (2003). Upper Ocean Control on the Solubility Pump of CO2. *J. Mar. Res.* 61, 465–489. doi:10.1357/002224003322384898

Jickells, T. D., An, Z. S., Andersen, K. K., Baker, A. R., Bergametti, G., Brooks, N., et al. (2005). Global Iron Connections between Desert Dust, Ocean Biogeochemistry, and Climate. *Science* 308 (5718), 67–71. doi:10.1126/science.1105959

Johnson, G. C., and Toole, J. M. (1993). Flow of Deep and Bottom Waters in the Pacific at 10°N. *Deep Sea Res. Oceanographic Res. Pap.* 40 (2), 371–394. doi:10.1016/0967-0637(93)90009-R

Kawabe, M., and Fujio, S. (2010). Pacific Ocean Circulation Based on Observation. *J. Oceanogr* 66 (3), 389–403. doi:10.1007/s10872-010-0034-8

Kawabe, M., Fujio, S., and Yanagimoto, D. (2003). Deep-Water Circulation at Low Latitudes in the Western North Pacific. *Deep Sea Res. Part Oceanographic Res. Pap.* 50 (5), 631–656. doi:10.1016/S0967-0637(03)00040-2

Kawahata, H., Suzuki, A., and Ohta, H. (1998). Sinking Particles between the Equatorial and Subarctic Regions (0°N-46°N) in the Central Pacific. *Geochem. J.* 32 (2), 125–133. doi:10.2343/geochemj.32.125

Kienast, S. S., Winckler, G., Lippold, J., Albani, S., and Mahowald, N. M. (2016). Tracing Dust Input to the Global Ocean Using Thorium Isotopes in marine Sediments: ThoroMap. *Glob. Biogeochem. Cycles* 30 (10), 1526–1541. doi:10.1002/2016GB005408

Kolla, V., Bé, A. W. H., and Biscaye, P. E. (1976). Calcium Carbonate Distribution in the Surface Sediments of the Indian Ocean. *J. Geophys. Res.* 81 (15), 2605–2616. doi:10.1029/JC081i015p02605

Laws, E. A., Falkowski, P. G., Smith, W. O., Jr, Ducklow, H., and McCarthy, J. J. (2000). Temperature Effects on export Production in the Open Ocean. *Glob. Biogeochem. Cycles* 14 (4), 1231–1246. doi:10.1029/1999GB001229

Li, L., Luo, Y., Kienast, M., Qi, D., and Tjiputra, J. (2021). On the Sedimentary Carbonate Accumulation and Dissolution in Western Pacific Marginal Basins. *Limnology and Oceanography* 67, 26–38. doi:10.1002/lno.11972

Liu, X., Luo, Y., and Boudreau, B. P. (2022). Effects of Deep Circulation on CaCO3 Dissolution and Accumulation in the Southwestern Atlantic Ocean. *Geophys. Res. Lett.* 49, e2021GL095020. doi:10.1029/2021GL095020

Millero, F. J. (1995). Thermodynamics of the Carbon Dioxide System in the Oceans. *Geochimica et Cosmochimica Acta* 59 (4), 661–677. doi:10.1016/0016-7037(94)00354-O

Olsen, A., Lange, N., Key, R. M., Tanhua, T., Bittig, H. C., Kozyr, A., et al. (2020). An Updated Version of the Global Interior Ocean Biogeochemical Data Product, GLODAPv2.2020. *Earth Syst. Sci. Data* 12 (4), 3653–3678. doi:10.5194/essd-12-3653-2020

Regnier, P., Friedlingstein, P., Ciais, P., Mackenzie, F. T., Gruber, N., Janssens, I. A., et al. (2013). Anthropogenic Perturbation of the Carbon Fluxes from Land to Ocean. *Nat. Geosci* 6 (8), 597–607. doi:10.1038/ngeo1830

Sarmiento, J. L., Dunne, J., Gnanadesikan, A., Key, R. M., Matsumoto, K., and Slater, R. (2002). A New Estimate of the CaCO3 to Organic Carbon export Ratio. *Glob. Biogeochem. Cycles* 16 (4), 54–15412. doi:10.1029/2002GB001919

Sexton, P. F., and Barker, S. (2012). Onset of 'Pacific-Style' Deep-Sea Sedimentary Carbonate Cycles at the Mid-Pleistocene Transition. *Earth Planet. Sci. Lett.* 321-322, 81–94. doi:10.1016/j.epsl.2011.12.043

Sulpis, O., Boudreau, B. P., Mucci, A., Jenkins, C., Trossman, D. S., Arbic, B. K., et al. (2018). Current CaCO3 Dissolution at the Seafloor Caused by Anthropogenic CO2. *Proc. Natl. Acad. Sci. U.S.A.* 115 (46), 11700–11705. doi:10.1073/pnas.1804250115

Tjiputra, J. F., Roelandt, C., Bentsen, M., Lawrence, D. M., Lorentzen, T., Schwinger, J., et al. (2013). Evaluation of the Carbon Cycle Components in the Norwegian Earth System Model (NorESM). *Geosci. Model. Dev.* 6 (2), 301–325. doi:10.5194/gmd-6-301-2013

Venzke, E. (2013). "Global Volcanism Program, 2013," in *Volcanoes of the World, v. 4.5. 2* (Washington, DC: Smithson. Institution, Natl. Museum Nat. Hist).

Volk, T., and Hoffert, M. I. (1985). "Ocean Carbon Pumps: Analysis of Relative Strengths and Efficiencies in Ocean-Driven Atmospheric CO2 Changes," in *The Carbon Cycle and Atmospheric CO2: Natural Variations Archean to Present*. Editors E. T. Sundquist and W. S. Broecker, 99–110. Washington, DC: American Geophysical Union (AGU). doi:10.1029/GM032p0099

Yu, J., Menviel, L., Jin, Z. D., Anderson, R. F., Jian, Z., Piotrowski, A. M., et al. (2020). Last Glacial Atmospheric CO2 Decline Due to Widespread Pacific Deep-Water Expansion. *Nat. Geosci.* 13 (9), 628–633. doi:10.1038/s41561-020-0610-5

Conflict of Interest: The authors declare that the research was conducted in the absence of any commercial or financial relationships that could be construed as a potential conflict of interest.

Publisher's Note: All claims expressed in this article are solely those of the authors and do not necessarily represent those of their affiliated organizations, or those of the publisher, the editors, and the reviewers. Any product that may be evaluated in this article, or claim that may be made by its manufacturer, is not guaranteed or endorsed by the publisher.

Copyright © 2022 Zhang, Che, Xia, Cheng, Qi, Cao and Luo. This is an open-access article distributed under the terms of the Creative Commons Attribution License (CC BY). The use, distribution or reproduction in other forums is permitted, provided the original author(s) and the copyright owner(s) are credited and that the original publication in this journal is cited, in accordance with accepted academic practice. No use, distribution or reproduction is permitted which does not comply with these terms.